Wireless Optical CDMA LAN: Digital Design Concepts

Babak M. Ghaffari, *Student Member, IEEE*, Mehdi D. Matinfar, *Student Member, IEEE*, and Jawad A. Salehi, *Senior Member, IEEE*

***Abstract*—In this paper we study and present an in-depth analysis on the operability and the viability of a typical wireless optical CDMA (OCDMA) local area network. Three receiver structures for OCDMA systems, using optical orthogonal codes (OOC) with minimum auto and cross-correlations as signature sequence, namely, correlation, correlation with hard-limiter, and chip-level detection are studied and proposed for such a network. For the synchronization circuit design the performance of two algorithms for OOC based OCDMA networks, namely, simple serial-search and multiple-shift in the context of wireless OCDMA LAN are studied. Furthermore, we study a synchronization method based on matched filtering and show that it presents a much better performance in our wireless OCDMA system. The effect of sampling rate and its performance on tracking circuit is analyzed. Bit-error-rate (BER) analysis is performed by photon counting methodology. Multi-user interference (MUI), ambient light, and photodetector dark current are considered in our analysis. Our analysis strongly indicates the viability and practicality of such systems in certain important wireless optical communications systems.**

***Index Terms*—OCDMA, wireless optical LAN, optical orthogonal codes, synchronization, acquisition, tracking, sampling effect.**

I. Introduction

WIRELESS local area networks have attracted an unexpected growth in research and development due to its feasibility, wide range of applications, market needs, and consumers' considerable demands. Consequently various standards have been developed for many specific applications and systems. Along with radio wireless LANs, optical wireless LANs are beginning to enjoy their special growth [1-3]. It is believed that wireless optical LANs will acquire in importance where security is of concern and where obtaining radio frequency band would not be economical. Furthermore optical wireless LANs are of immense interest in places such as hospitals and inside planes where electromagnetic interference is of utmost concern. And with progress in optical devices technologies considerable improvement in quality of service for these types of networks is within the reach [4-10].

In this paper we study and analyze practical digital designs in implementing a typical CDMA based infrared local area network prototype. Optical code division multiple-access (OCDMA) was first suggested for use in fiber-optic communications [11-14]. However, applying this technique to infrared media has been proposed recently [15-20]. This paper begins by studying and discussing the structures and principles of a wireless OCDMA LAN. In this system, all users communicate asynchronously. Optical Orthogonal Codes (OOCs) are used as the signature sequence to separate the active users' information. In this paper we assume a simple Line of Sight (LoS) model for the optical channel, and we focus on the performance of various types of OCDMA receivers using photon counting process. In the next part of this paper we consider a diffused or non-directed optical channel and the analysis takes into account the multipath effect and the corresponding channel models [5-8]. Optical transmitters and receivers considered here use Intensity Modulation/Direct Detection (IM/DD) technique with On-Off Keying (OOK) signaling for data communication.

In the analysis, the sampled value of the detected photons is assumed to be a random variable with Poisson distribution. The effect of background noise such as sunlight and florescent lights and also the effect of photodetector dark current on the system performance is obtained. The main difference between a fiber-optic and a wireless OCDMA receiver is that in the former the detection process can be performed in the optical domain. For example, optical hard-limiter can be placed in the path of incident optical signal. Also fiber tapped-delay lines can be designed to act as a correlator before photodetection. But in our wireless optical system which is implemented on a digital platform all detection operations including hard-limiting and correlation is performed after photodetection. For this reason we study various receiver structures proposed for fiber-optic CDMA that can be used in a typical indoor wireless optical network such as chip-level receiver and correlation + hard-limiter with sunlight, florescent lights, and photodetector dark current as the background noise. Synchronization circuitry which plays an important role in a typical CDMA receiver consists of acquisition and tracking blocks. In the acquisition stage the CDMA receiver is synchronized with an accuracy which is within half of chip time with its corresponding code in the start-up phase. The exact and dynamic synchronization is achieved during the tracking stage. Some algorithms have been proposed to be used in the acquisition block of an OCDMA receiver using OOC sequence [21-23]. In this paper we suggest one such acquisition technique namely match-filtering, and compare its performance with

Paper approved by W. C. Kwong, the Editor for Optical Networks of the IEEE Communications Society. Manuscript received September 4, 2006; revised February 10, 2007. This work was supported in part by Iran National Science Foundation (INSF).

The authors are with the Optical Networks Research Laboratory (ONRL), Electrical Engineering Department, Sharif University of Technology, Tehran, Iran (e-mail: babakghf@ieee.org, matinfar@ee.sharif.edu jasalehi@sharif.edu).

Digital Object Identifier 10.1109/TCOMM.2008.060495

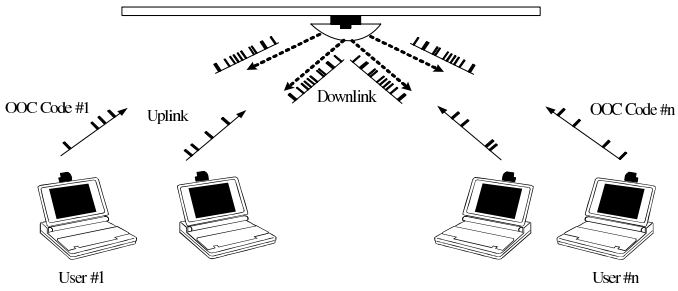

Fig. 1. A typical wireless OCDMA LAN containing a base station and n users.

simple and multiple-shift serial search algorithms. In a digital system, tracking circuit precision depends on the rate of the fastest achievable clock. Consequently, tracking action in digital systems may not be performed exactly as in some analog systems. Thereby we evaluate the effect of sampling on tracking operation and obtain the power penalty needed to mitigate this undesired effect.

The rest of this paper is organized as follows. In section II a typical wireless OCDMA network with three receiver structures in their digital forms are discussed. In section III we obtain expressions corresponding to BER for each receiver structure. Section IV describes and obtains the acquisition methods and their performance. In section V tracking circuit and the effect of sampling on its performance is discussed. Section VI concludes the paper.

II. System Description and Various Receiver Structures

It is almost impossible to implement an irregular and ad hoc network architecture for a wireless optical LAN due to the limitations of optical waves propagation properties. Especially, one or more base stations are needed to act as a bridge when a local network needs to be connected to a global network such as internet. Fig. 1 shows our system architecture which includes one base station, with a single pair of optical transmitter and receiver, and n user stations, each having a pair of optical transmitter and receiver.

With respect to the maximum number of permitted active users in the network and the desired code length, a set of OOCs is defined and each code is assigned to each active user. In this system each active user is assigned a signature sequence from a set of OOC which is specified by $(F, w, \lambda_a, \lambda_c)$, where F indicates the code length, w is the code weight, λ_a and λ_c are the maximum value allowed for autocorrelation and crosscorrelation of the code set in use. It is well known that the minimum value for λ_a and λ_c is equal to one due to the fact that in IM/DD format optical pulses are unipolar. For $\lambda_a = \lambda_c = 1$ the maximum number of codes in an OOC set, which limits the network capacity, is obtained as follows [11],

$$N \leq \left\lfloor \frac{F-1}{w\,(w-1)} \right\rfloor \tag{1}$$

Assuming each user's coded data as a binary stream we consider the downlink signal as the logically gated OR (summer + limiter) of all users' OOC coded data stream simultaneously which drives an optical transmitter such as a LED. So downlink can be considered as a synchronous OCDMA link.

Lemma 1: For an OOC set $(F, w, 1, 1)$, downlink multi-user interference can be omitted if $N < \frac{F}{w^2} + 1$.

Proof: Consider user 1 OOC code as the reference code. So, there are $F - w^2$ possible cyclic shifts for OOC code 2 in which there are no interference between code 1 and code 2. Likewise, there are $F - 2w^2$ possible cyclic shifts for OOC code 3 in which there are no interference between code 1, code 2, and code 3. Continuing this process if we have $F - (N-1)w^2 > 0$ then all the N OOC codes, each one with a proper cyclic shift, can be inserted into a F chips length frame such that no overlap, i.e., no interference, between them would exist.

Downlink Signal Channel

From the above lemma we can define the downlink signal to be as follows,

$$Y_{downlink}(t) = y^{(1)}_{downlink}(t) \vee y^{(2)}_{downlink}(t) \vee \ldots \vee y^{(N)}_{downlink}(t) \tag{2}$$

where $y^{(k)}_{downlink}$ is the kth user's downlink OOC signal and $\vee$ indicates the OR logic operation among the signals. Note that since downlink signal channel is based on synchronous OCDMA then all the elements that constitute $Y_{downlink}(t)$ are 0 or 1. By using OOK modulation each $y^{(k)}_{downlink}$ can be expressed as:

$$y^{(k)}_{downlink}(t) = \sum_{i=-\infty}^{\infty} \sum_{j=1}^{F} d_i^{(k)} c_j^{(k)} P_{T_c}\left(t - iT_b - jT_c\right) \tag{3}$$

where $\{d_i^{(k)}\}_i$ is downlink bit stream of user k with bit duration T_b and chip duration $T_c = T_b/F$, and $\{c_j^{(k)}\}_{j=1}^{F}$ denotes the kth OOC code pattern and $P_{T_c}(t)$ is a rectangular pulse defined as,

$$P_{T_c}(t) = \begin{cases} 1 & 0 \leq t < T_c \\ 0 & otherwise \end{cases} \tag{4}$$

Uplink Signal Channel

On the other hand in the uplink channel all active users send their data bits asynchronously on the common channel and therefore uplink signal is comprised from analog summation of all users' optical intensity transmitted signals. Hence, we can write the uplink signal as follows,

$$Y_{uplink}(t) = \sum_{k=1}^{N} y^{(k)}_{uplink}(t - \tau_k) \tag{5}$$

where $y^{(k)}_{uplink}(t)$ is uplink signal due to the kth user and τ_k indicates kth user delay time with respect to the base station reference clock and we have,

$$y^{(k)}_{uplink}(t) = \sum_{i=-\infty}^{\infty} \sum_{j=1}^{F} u_i^{(k)} c_j^{(k)} P_{T_c}\left(t - iT_b - jT_c\right) \tag{6}$$

where $\{u_i^{(k)}\}_i$ is uplink bit stream of user k.

In the design of any wireless CDMA communication network near-far problem needs to be addressed and for wireless OCDMA LAN the near-far problem and the required power control algorithms are discussed in [17]. From [17] the near-far problem in wireless OCDMA LAN requires specific

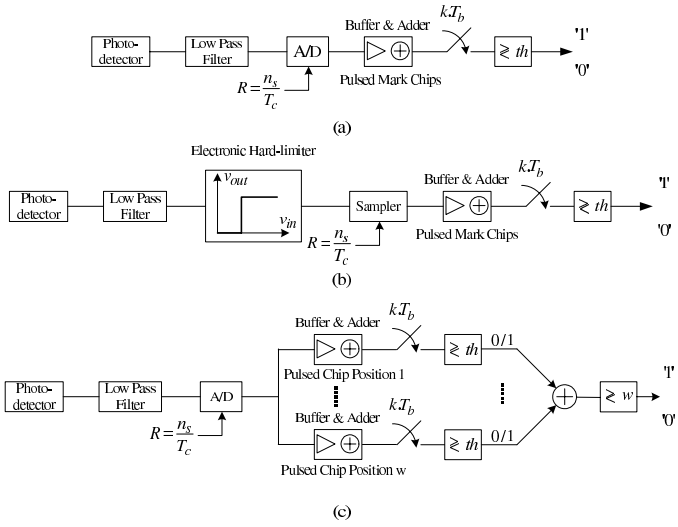

Fig. 2. Various digital structures for a wireless O-CDMA receiver (a) Correlator (b) Correlator + Hard-limiter (c) Chip-level detector.

algorithms to mitigate its effect such as the use of proper AGC circuit. Hence, in this paper we assume the existence of power control algorithms therefore we can safely ignore the near-far problem such that all users have equal power in the uplink channel. Appendix B discusses a methodology on power budget computation and obtains the minimum required power level of an optical transmitter that guarantees proper operation of a typical wireless OCDMA receiver.

In what follows we describe three viable and relevant receiver structures for a wireless OCDMA system, discuss their pros and cons in the context of digital design and implementation, and obtain their performance in both uplink and downlink channels and compare their performance.

A. Simple Correlator

Correlation receiver is the most propounded structure for OCDMA systems. This simple receiver involves a matched filter, corresponding to its code pattern, and an integrator followed by a sampler. In optical fiber CDMA systems the matched filter can be implemented by fiber tapped-delay lines at their receivers. However, in a typical wireless OCDMA LAN system where the speed of operation is not very high and the distances are relatively short correlation may take place after the photodetection at the receiver. In such a receiver the signal at the output of photodetector is sampled by an analog-to-digital converter (A/D) at a rate which is n_s times of the OOC chip rate, as shown in Fig. 2(a). The correlation of the received signal with the desired users' code can be evaluated by the summation of wn_s samples of received signal in all marked pulse chips of one bit duration using a simple adder. A buffer after the A/D operation saves the results of addition at each sampling time instant and resets at the end of the bit time. At the end of the bit duration, the accumulated value that is saved in the buffer, i.e., correlation value, is compared with an optimum threshold.

B. Correlator + Hard-limiter

It is shown that multi-user interference effect can be reduced by using an optical hard-limiter or optical AND logic gate in a fiber-optic CDMA receiver using unipolar codes such as OOCs, [11,13]. But as discussed before for our wireless OCDMA LAN receiver, the hard-limiter (electronic) is placed after the photodetector instead of being placed before the photodetector, Fig. 2(b). In our analysis, the electronic hard-limiter is modeled by a one-input one-output block with a predetermined threshold value. A simple hard limiting takes place using an analog circuit as shown in Fig. 2(b). Thus, each sample from wn_s samples has a binary value at the sampler output. The remaining operations are similar to the correlator receiver. In this structure, due to hard-limiting, the effect of multi-user interference is substantially reduced [25], as well as it simplifies the implementation since sampling operation can be done along with other processes for example in a Field Programmable Gate Array (FPGA) without using a separate A/D circuitry.

C. Chip-level Detector

Chip-level receiver was first introduced for fiber-optic CDMA [14] where decision is based upon each pulsed mark chip received power, constituting the desired OOC, instead of their combined power value. In this structure, the received power of each pulsed mark chip is compared with an optimum threshold. Bit '1' is decided if and only if all the w pulsed chips' power are greater than the optimum threshold otherwise bit '0' is decided. The notion and the operation of chip-level receiver is not the same as correlation and correlation + hard-limiter receiver, but its digital implementation is similar to correlation + hard-limiter structure. From a digital design point of view a decision on each pulsed mark chips is made based on the summation of each pulsed mark chip samples. Fig. 2(c) shows the operation of the chip-level detector. Each arm is dedicated for detecting one pulsed mark chip. At the first step the summation of the samples in each pulsed mark chip is evaluated by an adder and buffer in each arm. Finally, if all the resulting values due to w arms are greater than the optimum threshold bit '1' is decided otherwise bit '0' is decided.

III. BER Analysis

A. Simple Correlator

In this section we study and obtain the performance of the above mentioned receiver structures from digital design and implementational point of view. In digital structures, a low-pass filter followed by an analog to digital converter, A/D, are placed after the photodetector as discussed in section II. By assuming a low-pass filter with rectangular shape response equal to $P_{T_f}(t)$ with $T_f = T_c/n_s$, then the digital receiver acts as an integrate and dump circuit which is an optimum receiver for single user case in optical communication systems with Poisson channel [28]. Although, $n_s = 1$ is sufficient for chip-synchronous multi-user interference pattern for a proper detection, but for implementation purposes and for tracking circuitry we require to have more samples per chip as discussed in section V. However, for the sake of mathematical

simplicity and without any loss of generality we obtain the performance result on detection schemes for $n_s = 1$ and generalization to higher values of n_s will easily follow from the above simple case.

Let us consider $\vec{\alpha} = (\alpha_1, \alpha_2, ..., \alpha_w)$ as the interference pattern occurred on the pulsed mark chips. In other words α_j is the number of interferences on the jth pulsed mark chip of the desired OOC. In a simple correlator receiver structure the signal generated by integrate and dump circuit has a Poisson distribution function with a mean equal to [12],

$$m_d(l) = [(wd + l)\gamma_s + w\gamma_b]\ T_c \tag{7}$$

where $l = \sum_{j=1}^{w} \alpha_j$,$\gamma_s \equiv (\frac{2}{w})P_{av}\frac{\eta}{h\nu}$,$\gamma_b \equiv P_b\frac{\eta}{h\nu} + \frac{i_{dc}}{q}$, and $d \in \{0, 1\}$ indicates the transmitted data bit. P_{av} is the average received signal power on the photodetector area, P_b is ambient noise power, γ_s is the photoelectron count rate of received signal in a chip-time duration and γ_b is the sum of photoelectron count rate of background and dark current in a chip-time duration, i_{dc} and η are the photodetector dark current and quantum efficiency, respectively. Also q, ν , and h indicate electron charge, optical frequency, and Planck constant, respectively. To give an insight on the use of the above parameters, we assume the simplest possible case namely when there is no multiple-access interference, i.e., $N - 1 = 0$. For this case $m_1 = w(\gamma_s + \gamma_b)T_c$ and $m_0 = w\gamma_b T_c$, for on-off modulation. If we assume $P_b = -10.9\,dBm$, $P_{av} = -52\,dBm$ and $T_c = n_s T_f$ we have: $m_1 \cong 8.93722 \times 10^7$ and $m_0 \cong 8.90184 \times 10^7$. By Gaussian approximation and choosing optimum threshold the probability of error can be obtained as follows (see for example [28]):$P\,(error|ambient\ noise) \approx Q\left(\frac{m_1 - m_0}{\sqrt{m_1} + \sqrt{m_0}}\right) = Q\,(18.7) \to 0$

Note that in a typical indoor optical wireless channel, bandwidths are in the order of 10-40MHz [24]. For such low bandwidths in optical wireless channels, preamplifier's thermal noise can be ignored with respect to ambient noise [24]. We consider $I_b = 100\mu W/cm^2$ as the irradiance of ambient noise on the photodetector area. This value is typical for a receiver with optical bandwidth as high as 150nm, provided that it is placed in an environment without direct illumination of sunlight and without any incandescent lamps at the vicinity of the receiver [24]. P_b is related to I_b as $P_b = I_b A_d$ where A_d is the photodetector area.

For a correlator receiver the probability of error conditioned on l is obtained as follows,

$$P(E|l) = \frac{1}{2}g_{th}(m_0(l)) + \frac{1}{2} - \frac{1}{2}g_{th}(m_1(l)) \tag{8}$$

where,

$$g_{th}(x) = \sum_{n=th}^{\infty} \frac{x^n e^{-x}}{n!} \tag{9}$$

and th is an optimum threshold that minimizes the total probability of error. Total probability of error is computed by averaging over l as follows,

$$P_E = \sum_{l=0}^{N-1} P_l(N-1, l)P(E|l) \tag{10}$$

where l has a Bionomial distribution function for the uplink channel, [25]

$$P_l(N-1, l) = \binom{N-1}{l}\left(\frac{w^2}{2F}\right)^l\left(1 - \frac{w^2}{2F}\right)^{N-1-l} \tag{11.a}$$

In applying the condition of lemma 1, for the downlink channel we have,

$$P_l(N-1, l) = \delta(l) \tag{11.b}$$

where $\delta(\cdot)$ denotes Dirac delta function.

B. Correlator + Hard-limiter

For a receiver structure based upon a correlator with a hard-limiter, probability of error depends upon specific interference patterns instead of just the total number of interferences. In this structure we need to have two optimum thresholds instead of one as in simple correlator receiver. The first threshold, denoted as th_1, relates to the analog hard-limiter used right after the photodetector and the front and low-pass filter. It means that the average number of incident photons in each pulsed mark chip is compared to th_1 and a two-binary signal 0 or 1 will be generated. We show the output of analog hard-limiter by a w elements binary vector as $\vec{n} = (n_1, n_2, ..., n_w)$. Decision on the transmitted bit is based on the weight k of vector $\vec{n}$. If the weight k is greater than another optimum threshold, which we denote as th_2, then bit '1' is decided otherwise bit '0' is decided. In Appendix A, we show that for the correlator + hard-limiter receiver structure the probability of error conditioned on the interference pattern is as follows,

$$P(E|l, \vec{\alpha}) = \frac{1}{2}\sum_{k=th_2}^{w}\sum_{\vec{n}\in A_k}\prod_{j=1}^{w}\Big\{\left[g_{th_1}\left(m_0(\alpha_j)\right)\right]^{n_j} \times \left[1 - g_{th_1}\left(m_0(\alpha_j)\right)\right]^{(1-n_j)}\Big\} + \frac{1}{2} - \frac{1}{2}\sum_{k=th_2}^{w}\sum_{\vec{n}\in A_k}\prod_{j=1}^{w}\Big\{\left[g_{th_1}\left(m_1(\alpha_j)\right)\right]^{n_j} \times \left[1 - g_{th_1}\left(m_1(\alpha_j)\right)\right]^{(1-n_j)}\Big\} \tag{12}$$

Where A_k is the set of all w-element binary vectors,$\vec{n}$, with weight k. Note that the optimum thresholds are computed iteratively such that the whole probability of error is minimized. Also we have,

$$m_d(\alpha_j) = \left((d + \alpha_j)\gamma_s + \gamma_b\right)\ T_c\ \ ,\ \ d \in \{0, 1\} \tag{13}$$

which indicates the average number of incident photons on the jth pulsed mark chip assuming data bit $d \in \{0, 1\}$, and $\vec{\alpha} = (\alpha_1, \alpha_2, ..., \alpha_w)$ is the occurred interference pattern. Using (9) in (12) the probability of error for a correlator with a hard-limiter is computed as,

$$P_E = \sum_{l=0}^{N-1}\sum_{\vec{\alpha}\in B_l} P_l(l, \vec{\alpha})P(E|l, \vec{\alpha}) \tag{14}$$

Where B_l is the set of all interference patterns with l interfering users. The probability distribution function of interference pattern with $\vec{\alpha} = (\alpha_1, \alpha_2, ..., \alpha_w)$ and $l = \sum_{j=1}^{w}\alpha_j$ can be evaluated as follows,

$$P_l(l, \vec{\alpha}) = P_l(\vec{\alpha}|l)P_l(l, N-1) \tag{15}$$

TABLE I
SYSTEM PARAMETERS

F	OOC Length	128
w	OOC Weight	5
N	Active users number	4,5,6
n_s	Samples per chip	4
η	Photodetector quantum efficiency	0.8
λ	Optical wavelength	870 nm
I_b	Ambient light irradiance on the photodetector	100 $\mu W/cm^2$
i_d	Photodetector dark current	10 nA
A_d	Photodetector area	1 cm^2
T_f	Low pass filter response time	15.625 ns

$\vec{\alpha}$ can be produced in $\binom{l}{\alpha_1,\alpha_2,\ldots,\alpha_w} = \frac{l!}{\prod_{j=1}^{w}(\alpha_j)!}$ ways each with probability $\frac{1}{w^l}$ [12]. Thus for the uplink channel we have:

$$P_l(\vec{\alpha}|l) = \frac{l\,!}{w^l \prod_{j=1}^{w}(\alpha_j)!} \tag{16.a}$$

and for the downlink channel:

$$P_l(\vec{\alpha}|l) = \delta(\vec{\alpha}) \tag{16.b}$$

Finally, using (11.a), (11.b), (16.a) and (16.b) in (15) the probability distribution function of interference pattern is evaluated as follows for the uplink channel,

$$P_l(l,\vec{\alpha}) = \frac{(N-1)!}{w^l(N-1-l)!\prod_{j=1}^{w}(\alpha_j)!}\left(\frac{w^2}{2F}\right)^l\left(1-\frac{w^2}{2F}\right)^{N-1-l} \tag{17.a}$$

and for the downlink channel,

$$P_l(l,\vec{\alpha}) = \delta(l)\delta(\vec{\alpha}) \tag{17.b}$$

C. Chip-level Detector

In a chip-level structure, received power of each pulsed mark chips is compared with an optimum threshold. Bit '1' is decided if and only if all w pulsed chips' power are greater than an optimum threshold and '0' is decided otherwise. Following the analytical approach of the correlator with a hard-limiter, one can conclude that if the second threshold value in the correlator with a hard-limiter structure, th_2 , is replaced by the code weight, w, equations (12)-(17) are still valid for chip-level structure. However, the value of the first threshold, th_1 , for these two structures may not be the same.

Considering the parameters of Table I which correspond to a realistic scenario for multiple RS232 outputs (a low speed system), we have evaluated the analytical result of this section. Fig. 3 depicts the performance of the three above mentioned receivers' structure versus received average optical power, P_{av} , in uplink direction. We have considered 6 active users in this part of the analysis. As we can observe, the probability of error does not approach zero by increasing average optical power, since the number of active users are greater than the code weight which is equal to 5 in this example. Correlator + hard-limiter receiver obtains the best performance in signal

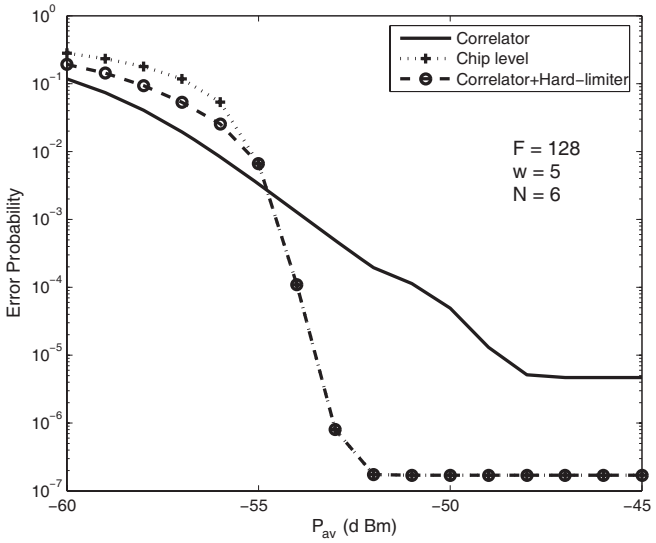

Fig. 3. Performance of various types of receivers vs. received optical power (uplink).

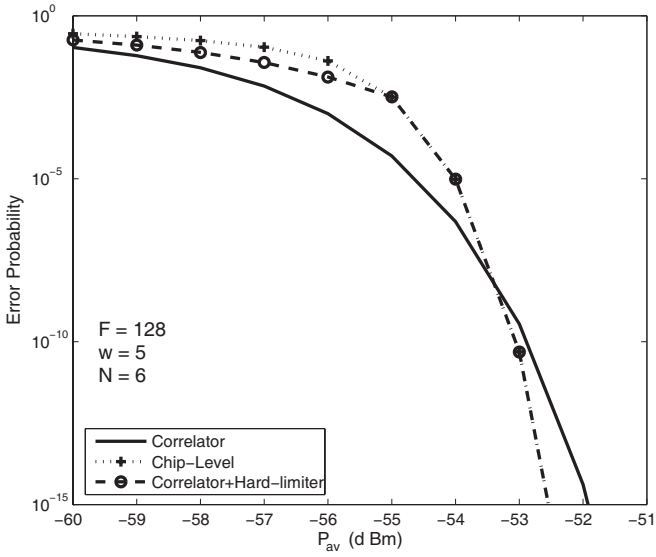

Fig. 4. Performance of various types of receivers vs. received optical power (downlink).

powers of practical interest when compared with other two receiver structures. For sufficiently high signal power, e.g., -55dBm and higher chip-level detector performance is fairly close to correlator + hard-limiter. On the other hand the simple correlator receiver obtains a better performance than correlator + hard-limiter and chip-level receivers, in the low average power region. But the increase in average received power P_{av}, which indicates stronger interfering users, then hard-limiter and chip-level receivers obtain better performance than the simple correlator, as it is shown in Fig. 3. By considering the results of Fig. 3, one can conclude that using chip-level or hard-limiter structure is a better choice than the correlator receiver specifically in the high signal power, i.e., $\geq -55dBm$. For $P_{av} = -52dBm$ we observe that the chip-level and hard-limiter structures present an improvement of about three orders of magnitude over correlation structure. Fig. 4 shows the performance of the above three receiver

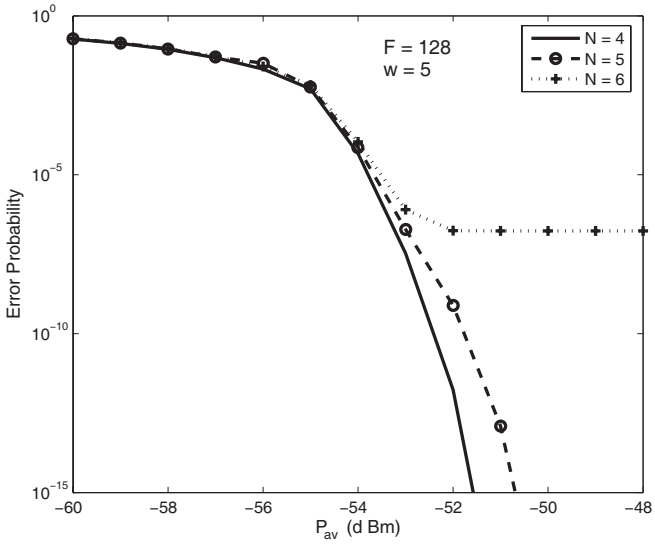

Fig. 5. Performance of correlator + hard limiter receiver vs. received average optical power and various number of users for uplink channel.

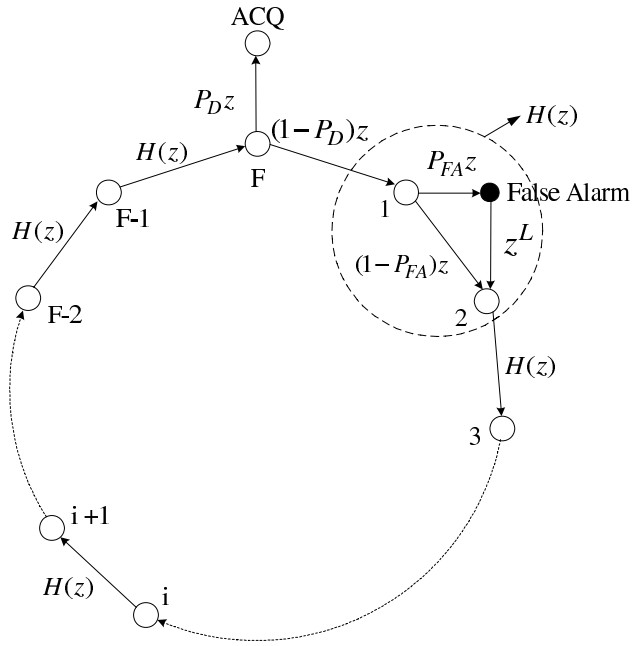

Fig. 6. Markov chain model for simple serial search algorithm

structures with the same parameters for downlink direction. The probability of error in this case is considerably lower than uplink channel since multi-user interference is omitted in downlink channel as described in section II. Only ambient light, shot noise effect, and dark current may cause errors in downlink direction. In Fig. 5 we depict the performance for various number of active users in the uplink channel for correlator + hard-limiter receiver. For $N = 4$ and $N = 5$ the probability of error approaches zero by increasing the received average optical power, since the number of interfering users is always lower than the code weight. However, with $N = 6$, probability of error approaches a floor limit due to multi-user interference effect.

IV. Acquisition Algorithms

In order to extract properly data bits from a spread stream of pulses, which constitutes the desired OOC receiver needs to know the correct initial reference time or the phase of the specified code pattern that carries the desired information bit. Assuming chip-synchronous, receiver encounters an ambiguity equal to F cells, each corresponding to one possible cyclic shift of the indicated OOC code. At the end of the acquisition level the correct cell, or equivalently the correct shift is found. This can be obtained for example by using training bits which are inserted at the beginning of each frame. Some algorithms are suggested to be used in acquisition state. For each algorithm, different number of training bits is required to meet acquisition with a probability near one. It is evident that the less training bits required the more efficient the algorithm in use will be. In the following we present three recently suggested algorithms for OOC based OCDMA and compare their performance from digital design point of view in a wireless OCDMA system.

A. Simple Serial-Search Method

In this approach, one cell is randomly selected and it is assumed to be the correct cell. A correlation between the received data and the selected code over a bit time duration (dwell time) is obtained and the outcome is compared with an optimum threshold. If the output of the correlation is greater than the optimum threshold, then the first randomly selected cell is the correct cell. Otherwise, we examine the next cell. By next cell we imply that a chip-sized rotation replica of the initial cell or phase of the specified code. So by continuing this algorithm and in maximum F stages we obtain the correct cell in the ideal case. Markov chain model simplifies the analysis of various acquisition algorithms. Such a model is depicted in Fig. 6 for the so called simple serial-search model. Each cell is represented by a node. Here we assume that the correct cell is the Fth cell. P_D is the probability of correct detection. Transmission between each two cells is represented by a transfer function with parameter z. The power of z indicates delay in bit duration (T_b). So we observe that the transfer function of correct decision on correct cell is $P_D z$ and incorrect decision is $(1 - P_D)\, z$. P_D is not equal to 1 in the real case due to shot noise effect. Transfer function between each two incorrect cells is defined as $H(z)$. Also we denote the false alarm probability by P_{FA}. When correlation on an incorrect shift exceeds optimum threshold a false alarm is occurred. P_{FA} is not equal to zero because of multiple-access interference and environmental noise effects. L indicates the time that the tracking circuit requires to recognize false decision in an acquisition block. According to figure 6 transfer function between each two incorrect cells is as follows [21],

$$H(z) = (1 - P_{FA})\, z + P_{FA} z^{L+1} \tag{18}$$

If $U_i(z)$ denotes the transfer function from cell i to correct cell, $U(z)$ is obtained by averaging over $U_i(z)$ for $i = 1, 2, \ldots, F$. It is shown that the average time to reach the correct cell is as follows,

$$E\{N_{ACQ}\} = \frac{d\,U(z)}{d\,z}|_{z=1} \tag{19}$$

Using the result of [21] for OOC based OCDMA system we have,

$$E\{N_{ACQ}\} = \frac{F-1}{2}(P_{FA}L-1) + \frac{1}{P_D}\left[F + L(F-1)(1-P_D)P_{FA}\right] \quad (20)$$

Considering correlator structure, P_D and P_{FA} are probabilities of correct detection and false alarm conditioned on bit '1' respectively. So using (8)-(11) and according to [21], these parameters can be computed as follows,

$$P_D = \sum_{l=0}^{N} P_l(N,l)\, g_{th}(m_1(l)) \quad (21.a)$$

$$P_{FA} = \sum_{l=0}^{N} P_l(N,l)\, g_{th}(m_0(l)) \quad (21.b)$$

where $g_{th}(x)$ and $P_l(N,l)$ are defined in (9) and (11), respectively. The threshold th is computed iteratively such that $E\{N_{ACQ}\}$ achieves its minimum possible value.

B. Multiple-shift Method

To reduce average time of acquisition, multiple-shift method was proposed recently [22]. In this method F cells are divided into Q groups each containing M cells. In the first stage of the algorithm, all M cells of group 1 are examined simultaneously. If the output of the correlation is greater than a predetermined optimum threshold then we proceed to second stage, otherwise examine cells which belong to group 2. In continuing this process and from [22] in maximum Q steps we obtain the true group. In the second stage the M possible cells will be examined one by one similar to the simple serial-search method. Fig. 7 shows Markov diagram for multiple-shift method. Assuming that the Qth group contains the correct cell then the transfer functions $H(z)$ and $h(z)$, between two incorrect node in the first and second stage respectively, are computed as follows,

$$H(z) = (1-P_{FA})z + P_{FA}z\,h^M(z) \quad (22)$$

$$h(z) = (1-p_{fa})z + p_{fa}z^{L+1} \quad (23)$$

Note that in (22) and (23) capital letters refer to the first stage and small letters refer to the second stage respectively. Assuming that we have found the correct group then similar to simple serial-search method an initial random phase v is then selected. The other transfer functions that are needed to describe multiple-shift method are $H_{det}(z)$ and $H_{miss}(z)$, the former being the transfer function from node Q to acquisition state and the latter being the transfer function from node Q to node 1. Considering Fig. 7 and using (19) then the average number of the training bits is computed as,

$$\mathrm{E}(N_{Acq}) = \frac{H'_{det}(1) + H'_{miss}(1)}{p_d P_D} + (Q-1)H'(1)\frac{2-p_dP_D}{2p_dP_D} \quad (24)$$

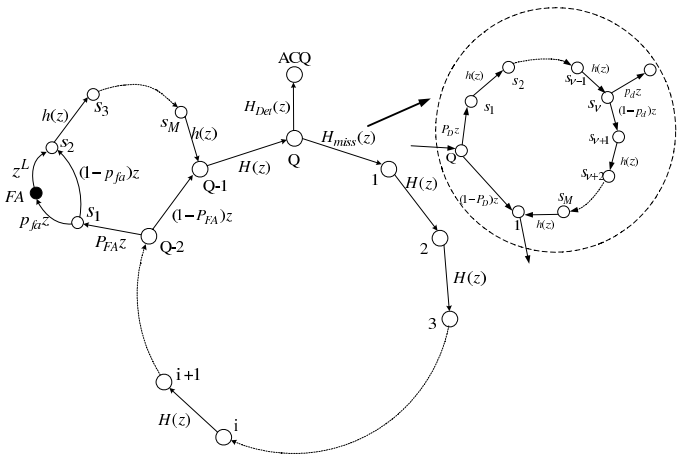

Fig. 7. Markov chain model for Multiple-shift algorithm

where

$$H'(1) = 1 + M\,P_{FA}(1 + L\,p_{fa}) \quad (25.a)$$

$$H'_{det}(1) = \frac{1}{2}p_dP_D[(M+3) + L(M-1)p_{fa}] \quad (25.b)$$

$$H'_{miss}(1) = (1-P_D) + P_D(1-p_d)[M+1+L(M-1)p_{fa}] \quad (25.c)$$

Considering a correlator structure and from [22], P_D, p_d, P_{FA} and p_{fa} can be computed as follows,

$$P_D = \sum_{l=0}^{NM} P_l(NM,l)\, g_{TH}(l, m_1(l)) \quad (26.a)$$

$$p_d = \frac{1}{P_D}\sum_{l_1=0}^{N}\sum_{l=0}^{N(M-1)} \{P_l(N,l_1)P_l(N(M-1),l)\} \times \{g_{th}(m_1(l_1))\, g_{th}(m_1(l))\} \quad (26.b)$$

$$P_{FA} = \sum_{l=0}^{NM} P_l(NM,l)\, g_{TH}(m_0(l)) \quad (26.c)$$

$$p_{fa} = \frac{1}{P_{FA}}\sum_{l_1=0}^{N}\sum_{l=0}^{N(M-1)} \{P_l(N,l_1)P_l(N(M-1),l)\} \times \{g_{th}(m_0(l_1))\, g_{th}(m_0(l))\} \quad (26.d)$$

where TH and th indicate the first and second stage thresholds respectively and their values are defined such that $E\{N_{ACQ}\}$ obtained from (24) achieves it's minimum value.

C. Match-Filter Method

Assume a match-filter containing w delay lines. Each, delay line value is proportional to the position of pulsed chips corresponding to its respective OOC. When training bits enter the match-filter then the output signal is a periodic training pulse with a width equal to T_c and a period equal to T_b. This implies that in one bit duration we can observe the peak correlation of the incident signal and code pattern without any knowledge of the correct initial time reference. As an example we depict the digital implementation of a match-filter for an OOC stream with $w = 3$ in Fig. 8. Considering this idea, match-filtering automatically searches all the F cells within

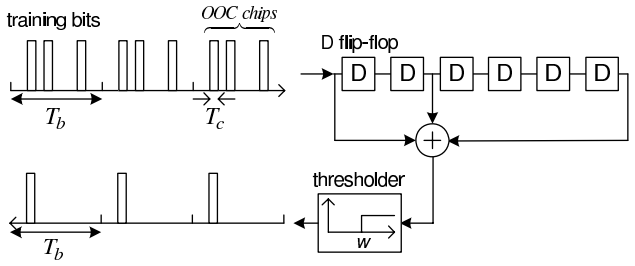

Fig. 8. An example of digital match-filter for an OOC stream with w=3.

one bit duration instead of F bits duration as in the simple serial-search method. The Markov chain model is similar to that represented for simple serial-search method, Fig. 6, except that the dwell time in serial-search method is equal to one bit duration, T_b, but in the match-filter method the dwell time is reduced to chip duration, $T_c = T_b/F$. According to Fig. 6 and (16), the transfer function $H(z)$ for match-filter method is,

$$H(z) = (1 - P_{FA})\, z^{1/F} + P_{FA} z^{L+(1/F)} \tag{27}$$

Inserting (27) in (18) and using (19) we have,

$$E\{N_{ACQ}\} = \frac{1}{P_D} - \frac{F-1}{2F} + L\left(\frac{1-P_D}{P_D}\right)(F-1)\,P_{FA} + L\left(\frac{F-1}{2}\right)P_{FA} \tag{28}$$

In Fig. 9 we have depicted the required average number of training bits for the above three mentioned algorithms. Match-filter method presents a more efficient algorithm than the other two methods. Specifically, in relatively high received power region one bit is sufficient to acquire acquisition. For multiple-shift algorithm the optimum value for M is five for nominal values given in table I. Although multiple-shift method is not as efficient as match-filter, but it represents a more efficient algorithm when compared to simple serial-search method.

V. Digital Tracking Circuit

Tracking circuit performs two key operations in a typical OCDMA receiver. In general, the received code from acquisition block has an ambiguity in phase or initial time reference which is less than $T_c/2$. The first task of the tracking circuit is to minimize this ambiguity. Digital tracking accuracy depends on the systems fastest clock speed. The second task for the tracking circuit is to alarm the *out of synchronization state* to the acquisition block. We choose early-late method for digital implementation of the tracking circuit [26]. In this method two separate early and late replica of the reference code, which is produced by the acquisition block, is generated by the tracking block. If $c(t)$ denotes the reference code, then $c(t + T_c/2)$ and $c(t - T_c/2)$ are the corresponding early and late codes, respectively. Now, correlation action takes place between the training bit stream and the early and late codes. If the output of both early and late correlators are less than a threshold that is determined by the detection block and is computed such that (10) is minimized for L sequential bits, then "synchronization out" signal is activated. This signal is passed to the acquisition block to switch on the acquisition

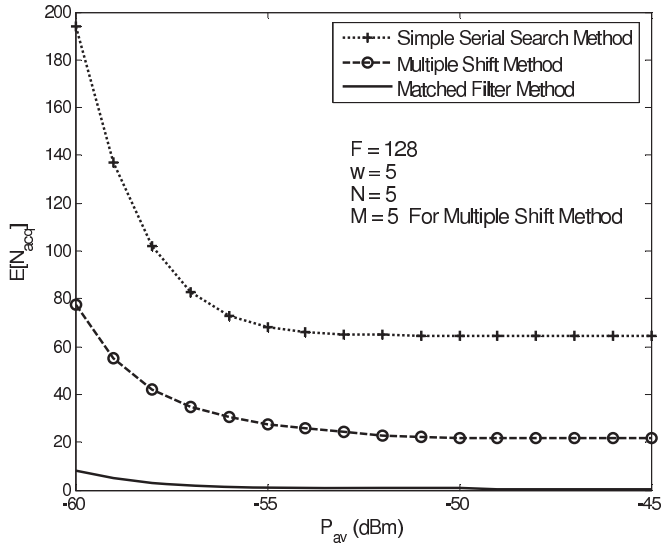

Fig. 9. Average number of training bits required for various types of acquisition algorithms

state. To track the original code, the values of early and late correlator outputs are subtracted, and three actions may be initiated based on the subtraction result. Selecting a proper threshold, say th_c, then a shifted replica to the correlator is selected as the new reference code if the subtraction result is greater than th_c. A shifted replica to the late correlator is selected if subtraction result is less than $-th_c$, otherwise the main code is selected. To select the proper threshold value, th_c, we need to consider two main issues namely th_c value must not be so low in order to cause the tracking circuit to oscillate and not so high in order for tracking circuit not be able to follow the phase shifts fluctuations.

Furthermore, the sampling rate dramatically affects the performance of tracking circuit. For very high value of the sampling rate, digital tracking circuit operation is then fairly equal to an analog circuit. But in the real cases, the fastest clock speed of the system limits the number of samples per chip. To evaluate the effect of sampling on the tracking operation, and consequently on the system performance, we need to consider interferences on the first cyclic shift of the desired code as well as interferences on the original phase of the desired code. In this way, for a correlator structure we show the number of interferences on the desired code by l_1 and the number of interferences on the first cyclic shift of the desired code by l_2. In general the two random variables l_1 and l_2 are dependent, therefore their joint probability density function is required for BER analysis of the tracking circuit. To obtain the joint probability density function of l_1 and l_2 we need to know all the possible code patterns in the system which prove to be mathematically tedious and impractical. Let us assume as in [22], as a simplifying approximating assumption that random variables l_1 and l_2 are independent. Also we assume that the offset of tracking circuit reference code and the original phase of the desired code is equal to τ. Then the average photon counts that is generated by correlating the incident signal and the tracking reference code is as follows,

$$m_d(l_1, l_2, \tau) = (w\gamma_b + l_2\gamma_s)\tau +$$

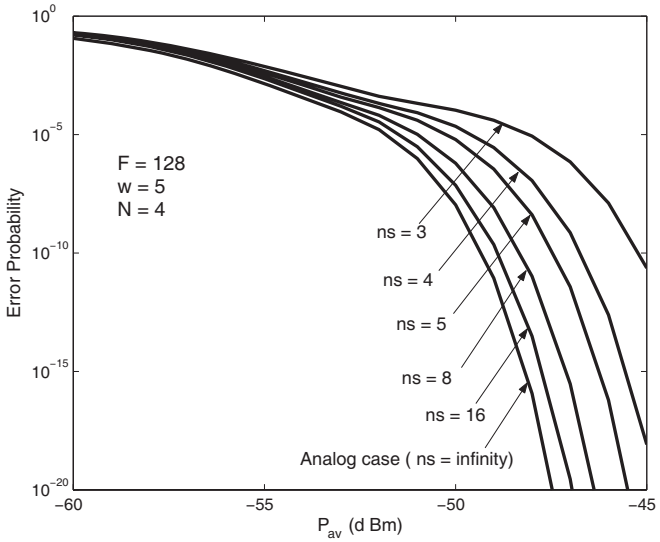

Fig. 10. Effect of sampling on the system performance

$$[w\gamma_b + (l_1 + wd)\gamma_s]\ (T_c - \tau)\ \ ,\ \ d \in \{0, 1\} \tag{29}$$

To compute probability of error conditioned on l_1, l_2 and τ we can write,

$$P(E|l_1, l_2, \tau) = \frac{1}{2} g_{th}\left[m_0(l_1, l_2, \tau)\right] + \frac{1}{2} - \frac{1}{2} g_{th}\left[m_1(l_1, l_2, \tau)\right] \tag{30}$$

$g_{th}(x)$ is defined in (9) and th denotes the optimum threshold for the tracking circuit. The total probability of error, conditioned on τ, is computed as follows,

$$P_E(\tau) = \sum_{l_1=0}^{N-1} \sum_{l_2=0}^{N-1} P_{l_1}(N-1, l_1) P_{l_2}(N-1, l_2) P(E|l_1, l_2, \tau) \tag{31}$$

$P_l(N-1, l)$ is defined in (11) for uplink and downlink directions. Assuming a sampling rate of n_s/T_c then the offset of tracking reference code and original code can be up to T_c/n_s. Hence, to obtain probability of error, P_E, we need to take an average over τ on (31) over the interval $[0, T_c/n_s]$. Assuming a uniform distribution for offset value we can write,

$$P_E = \frac{n_s}{T_c} \int_0^{T_c/n_s} P_E(\tau)\, d\tau \tag{32}$$

Fig. 10 shows the effect of sampling rate on the system performance for uplink direction. The results obtained are for a correlator receiver with several values of sampling rate per chip. From Fig. 10, we clearly observe that an increase in sampling rate the digital system performance approaches that of a perfect analog tracking circuit as expected.

VI. Conclusion

We evaluated the performance of various types of digital receivers in a typical wireless OCDMA indoor local area network based on photon counting process. Considering the implementation criteria, digital structures were introduced. The results show that correlation with hard-limiter not only obtains the best performance among other receiver structures such as the simple correlator and chip-level receivers it also constitutes a simple implementational structure. However chip-level detection performance approaches that of correlation with hard-limiter in high power region. Three algorithms proposed for acquisition circuit are studied using correlator structure. We show that match-filter method is the superior algorithm in reducing the number of required training bits. Also we evaluated the performance of digital tracking circuit in a wireless OCDMA environment. In our performance evaluation we considered the effect of the sampling rate on its performance. The results obtained for the various stages of the proposed wireless OCDMA LAN strongly indicate the operability and viability of such networks in certain applications.

Appendix A

In this appendix, we obtain eq. (12). The probability of error, conditioned on l (the number of interferences) and $\vec{\alpha}$ the interference pattern, can be expressed as follows:

$$\begin{aligned} P(E|l, \vec{\alpha}) =& P(d=0) P(E|d=0, l, \vec{\alpha}) \\ &+ P(d=1) P(E|d=1, l, \vec{\alpha}) \end{aligned} \tag{A.1}$$

Where d indicates the transmitted information bit. Assuming equal probability for transmitting bit '1' and '0' and indicating the decided bit with parameter r we can write:

$$\begin{aligned} P(E|l, \vec{\alpha}) =& \frac{1}{2} P(r=1|d=0, l, \vec{\alpha}) \\ &+ \frac{1}{2}\left(1 - P(r=1|d=1, l, \vec{\alpha})\right) \end{aligned} \tag{A.2}$$

As discussed in section (III.B), the output of the hard-limiter in one bit duration is denoted by a w-element binary vector $\vec{\alpha}$. If the weight of this vector is greater than th_2, bit '1' is decided, therefore:

$$\begin{aligned} P(r=1|d, l, \vec{\alpha}) =& P(\sum_{j=1}^{w} n_j \geq th_2 | d, l, \vec{\alpha}) \\ =& \sum_{k=th_2}^{w} P(\sum_{j=1}^{w} n_j = k | d, l, \vec{\alpha}) \end{aligned} \tag{A.3}$$

Let, A_k denote the set of all w-element binary vectors with weight k, then:

$$P(\sum_{j=1}^{w} n_j = k | d, l, \vec{\alpha}) = \sum_{\vec{n} \in A_k} P(n_1, n_2, ..., n_w | d, l, \vec{\alpha}) \tag{A.4}$$

Let s_j denote the number of photoelectrons in the jth pulsed mark chips, then:

$$\begin{aligned} P(n_j = 1|d, l, \vec{\alpha}) &= P(s_j \geq th_1 | d, l, \vec{\alpha}) = g_{th_1}\left(m_d(\alpha_j)\right) \\ P(n_j = 0|d, l, \vec{\alpha}) &= 1 - g_{th_1}\left(m_d(\alpha_j)\right) \end{aligned} \tag{A.5}$$

The generalized form for the above equations is as follows,

$$P(n_j|d, l, \vec{\alpha}) = \left[g_{th_1}\left(m_d(\alpha_j)\right)\right]^{n_j} \left[1 - g_{th_1}\left(m_d(\alpha_j)\right)\right]^{(1-n_j)} \tag{A.6}$$

Since random variables $\{s_j\}_{j=1}^{w}$ conditioned on l and $\vec{\alpha}$ are mutually independent it implies that the random variables $\{n_j\}_{j=1}^{w}$ are also independent and we can write:

$$P(n_1, n_2, n_3, ..., n_w | d, l, \vec{\alpha}) = \prod_{j=1}^{w} \left[g_{th_1}\left(m_d(\alpha_j)\right)\right]^{n_j} \left[1 - g_{th_1}\left(m_d(\alpha_j)\right)\right]^{(1-n_j)} \quad \text{(A.7)}$$

Inserting (A.7) in (A.4) and using (A.3) and (A.2) equation (12) is obtained.

APPENDIX B

In this appendix we discuss the methodologies used to obtain the minimum power level of an optical transmitter that guarantees proper operation of a typical short range wireless OCDMA receiver in the presence of multi-user interference signal. For the optical transmitter module we consider a fast LED with a relatively wide angle for optical transmission. The operational wavelength for the above LED is 870 nm and its propagation pattern is Lambertian with a half-angle $\theta_{1/2}$ equal to 15 degrees. Using a proper driver circuit, the LED can generate narrow optical pulses with a peak power as high as 400 mW. For optical receiver module we consider a PIN photodiode with an operational wavelength which is compatible to LED's in use. An optical lens with a $1cm^2$ effective area is mounted over this PIN photodiode. In order to obtain the required power for each chip of the coded data stream we use a set of OOC with length equal to 128 and weight equal to 5 to encode the OOC's pulses. The number of active users is equal to 4 and Tx-Rx distance has a range of 0.5 to 3 meters. Power budget is obtained under two conditions. First, we must consider IEC's class A standard to meet eye-safety conditions [27]. Second, in the worst case misalignment for Tx-Rx from the ideal line of sight in the presence of all interfering users, system must operate at a BER less than 10^{-9}. In this case we consider received optical power as follows [3],

$$P_r = \left(\frac{P_t\, R(\theta, \phi)}{d^2}\right) A_{eff} \quad \text{(B.1)}$$

where P_t and d are transmitted optical power and Tx-Rx distance, respectively. A_{eff} indicates lens effective area which is considered $1cm^2$ in our analysis, and $R(\theta, \phi)$ is the propagation pattern function of LED. θ and ϕ are the elevation and azimuth angles, respectively. The propagation function of a Lambertian source with order m is defined as [3],

$$R(\theta, \phi) = \frac{m+1}{2\,\pi} \cos^m \theta \quad \text{(B.2)}$$

If propagation half-angle of optical transmitter is equal to $\theta_{1/2}$ then m is obtained as follows,

$$m = \frac{\ln(1/2)}{\ln(\cos\ \theta_{1/2})} \quad \text{(B.3)}$$

For a correlator structure with hard-limiter, to obtain a BER less than 10^{-9}, the received optical power P_r needs to be at least $-52dBm$. For the worst case scenario we assume Tx-Rx distance and misalignment, to be $d = 3\ m$ and $\theta = 30^\circ$ respectively. For the above mentioned LED we have $\theta_{1/2} = 15^\circ$ and using (B.3) Lambertian order m is equal to 20. Using (B.2) $R(\theta, \phi) = 0.188$ for the worst case. From (B.1) we obtain $P_t = 3.01mW$ which is the average transmitted optical power per bit. Using results of [27] we observe that maximum allowable transmission power for a typical optical transmitter operating at 870 nm and a 15° propagation half-angle is equal to $28mW$. Hence, our optical transmitter meets class *A* standard of IEC. To compute optical power for each OOC chip pulse in an infrared CDMA transmitter we can write,

$$P_{t/OOC\ chip\,pulse} = \frac{2F}{w} P_t \quad \text{(B.4)}$$

where F and w are OOC code length and weight, respectively. So optical power per chip is $154mW$, which is less than maximum achievable power, i.e., $400mW$, of the above mentioned LED.

REFERENCES

[1] F. R. Gfeller and U. H. Bapst, "Wireless in-house data communication via diffuse infrared radiation," *Proc. IEEE*, vol. 67, no. 11, pp. 1474–1486, Nov. 1979.

[2] J. R. Barry, *Wireless Infrared Communications*. Boston: Kluwer, 1994.

[3] J. M. Kahn and J. R. Barry, "Wireless infrared communications," *Proc. IEEE*, vol. 85, no. 2, pp. 265–298, Feb. 1997.

[4] M. Abtahi and H. Hashemi, "Simulation of indoor propagation channel at infrared frequencies in furnished office environments," in *Proc. Sixth IEEE International Symposium on Personal, Indoor and Mobile Radio Communications 1995 (PIMRC'95)*, vol. 1, pp. 306–310, Sept. 1995.

[5] M. R. Pakravan and M. Kavehrad, and H. Hashemi, "Indoor wireless infrared channel characterization by measurements," *IEEE Trans. Veh. Technol.*, vol. 50, no. 4, pp. 1053–1073, July 2001.

[6] H. Hashemi, Yun Gang, M. Kavehrad, F. Behbahani, and P. A. Galko, "Indoor propagation measurements at infrared frequencies for wireless local area networks applications," *IEEE Trans. Veh. Technol.*, vol. 43, no. 3, Part 1-2, pp. 562–576, Aug. 1994.

[7] S. Jivkova and M. Kavehrad, "Receiver designs and channel characterization for multi-spot high-bit-rate wireless infrared communications," *IEEE Trans. Commun.*, vol. 49, no. 12, pp. 2145–2153, Dec. 2001.

[8] J. B. Carruthers and J. M. Kahn, "Modeling of nondirected wireless infrared channels," *IEEE Trans. Commun.*, vol. 45, no. 10, pp. 1260–1268, Oct. 1997.

[9] K. Akhavan, M. Kavehrad, and S. Jivkova, "High-speed power-efficient indoor wireless infrared communication using code combining .I," *IEEE Trans. Commun.*, vol. 50, no. 7, pp. 1098–1109, July 2002.

[10] M. Kavehrad and S. Jivkova, "Indoor broadband optical wireless communications: optical subsystems designs and their impact on channel characteristics," *IEEE Trans. Wireless Commun.*, vol. 10, no. 2, pp. 30–35, Apr. 2003

[11] J. A. Salehi, "Code division multiple-access techniques in optical fiber networks—part I: fundamental principles," *IEEE Trans. Commun.*, vol. 37, pp. 824–833, Aug. 1989.

[12] S. Zahedi and J. A. Salehi, "Analytical comparison of various fiber-optic CDMA receiver structures," *IEEE J. Lightwave Technol.*, vol. 18, no. 12, pp. 1718–1727, Dec. 2000.

[13] S. Mashhadi and J. A. Salehi, "Code division multiple-access techniques in optical fiber networks—part III: optical AND gate receiver structure with generalized optical orthogonal codes," *IEEE Trans. Commun.*, vol. 45, pp. 1457–1468, Aug. 2006.

[14] H. M. H. Shalaby, "Chip level detection in optical code division multiple access," *J. Lightwave Technol.*, vol. 16, pp. 1077–1087, June 1998.

[15] J. M. Elmirghani and R. A. Cyran, "Indoor 1nfrared wireless networks utilizing PPM-CDMA," in *Proc. ICCS*, pp. 334–337, 1994.

[16] S. Zahedi and J. A. Salehi, "M-Ary infrared CDMA for indoors wireless communications," in *Proc. IEEE PIMRC' 01*, vol. 2, pp. 6–10, Sept./Oct. 2001.

[17] A. Aminzadeh-Gohari and M. R. Pakravan, "Analysis of power control for indoor wireless infrared CDMA communication," in *Proc. 25th IEEE International Conference on Performance, Computing, and Communications Conference (IPCCC 2006)*, Apr. 2006.

[18] R. Vento, J. Rabadan, R. Perez-Jimenez, A. Santamaria, and F. J. Lopez-Herandez, "Experimental characterization of a direct sequence spread spectrum system for in-house wireless infrared communications," *IEEE Trans. Consumer Electron.*, vol. 45, no. 4, pp. 1038–1045, Nov. 1999

[19] K. K. Wong and T. O'Farrell, "Spread spectrum techniques for indoor wireless IR communications," *IEEE Wireless Commun.* , vol. 10, no. 2, pp. 54–63, Apr. 2003.
[20] X. N. Fernando, "Performance of an infrared wireless CDMA system," in *Proc. Digital Wireless Communication V* at SPIE's 17th Annual Aerosense Symposium, pp. 412–417, Apr. 2003.
[21] A. Keshavarzian and J. A. Salehi, "Optical orthogonal code acquisition in fiber-optic CDMA systems via the simple serial-search method," *IEEE Trans. Commun.*, vol. 50, no. 3, pp. 473–483, Mar. 2002.
[22] A. Keshavarzian and J. A. Salehi, "Multiple-shift code acquisition of optical orthogonal codes in optical CDMA systems," *IEEE Trans. Commun.*, vol. 53, no. 4, pp. 687–697, Apr. 2005.
[23] M. M. Mustapha and R. F. Ormondroyd, "Performance of a serial-search synchronizer for fiber-based optical CDMA systems in the presence of multi-user interference," in *Proc. SPIE*, vol. 3899, pp. 297–306, Nov. 1999.
[24] R. Otte, L. P. de Jong, and A. H. M. van Roermund, *Low-Power Wireless Infrared Communications*. Boston: Kluwer Academic Publishers, 1999.
[25] J. A. Salehi and C. A. Brackett, "Code division multiple-access techniques in optical fiber networks—part II: system performance analysis," *IEEE Trans. Commun.*, vol. 37, pp. 834–842, Aug. 1989.
[26] R. L. Peterson, D. E. Borth, and R. E. Ziemer, *Introduction to Spread Spectrum Communications*. Prentice-Hall, 1995.
[27] Int. Electrotech. Commission, *CEI/IEC 825-1: Safety of Laser Products*, 1993. J. D. Rancourt, *Optical Thin Film*. New York: Macmillan, 1987.
[28] R. M. Gagliardi and S. Karp, *Optical Communications*. John Wiley, 1995.

Babak M. Ghaffari (S'06) was born in Tehran, Iran, on February 18, 1978. He received the B.S. and M.S. degrees in electrical engineering from Sharif University of Technology (SUT), Tehran, in 2000 and 2002 respectively. He is currently working toward the Ph.D. degree in the Department of Electrical Engineering at SUT. Since 2002 he has been with Optical Networks Research Lab (ONRL) as a member of technical staff. His research interests include wireless optical and fiber-optic communication systems, optical CDMA and multiple-access communications.

Mehdi D. Matinfar (S'06) was born in Tehran, Iran, on May, 1980. He received the B.S. degree in electrical engineering from Sharif University of Technology (SUT), Tehran, in 2002 and the M.S. degree in electrical engineering from Khajeh Nasir University of Technology (KNUT), Tehran, in 2004. He is currently working toward the Ph.D. degree in the Department of Electrical Engineering at SUT. From June 2001 to September 2002, he was a member of Research Staff of the Mobile Communications Division at Iran Telecommunication Research Center (ITRC), and since 2003 he has been with Optical Networks Research Lab (ONRL) as a member of technical staff. His research interests include wireless communication systems and optical communication systems, specifically, optical CDMA and indoor optical communications.

Jawad A. Salehi (M'84-SM'07) was born in Kazemain, Iraq, on December 22, 1956. He received the B.S. degree from the University of California, Irvine, in 1979, and the M.S. and Ph.D. degrees from the University of Southern California (USC), Los Angeles, in 1980 and 1984, respectively, all in electrical engineering. He is currently a Full Professor at the Optical Networks Research Laboratory (ONRL), Department of Electrical Engineering, Sharif University of Technology (SUT), Tehran, Iran, where he is also the Co-Founder of the Advanced Communications Research Institute (ACRI). From 1981 to 1984, he was a Full-Time Research Assistant at the Communication Science Institute, USC. From 1984 to 1993, he was a Member of Technical Staff of the Applied Research Area, Bell Communications Research (Bellcore), Morristown, NJ. During 1990, he was with the Laboratory of Information and Decision Systems, Massachusetts Institute of Technology (MIT), Cambridge, as a Visiting Research Scientist. From 1999 to 2001, he was the Head of the Mobile Communications Systems Group and the Co-Director of the Advanced and Wideband Code-Division Multiple Access (CDMA) Laboratory, Iran Telecom Research Center (ITRC), Tehran. From 2003 to 2006, he was the Director of the National Center of Excellence in Communications Science, Department of Electrical Engineering, SUT. He is the holder of 12 U.S. patents on optical CDMA. His current research interests include optical multiaccess networks, optical orthogonal codes (OOC), fiber-optic CDMA, femtosecond or ultrashort light pulse CDMA, spread-time CDMA, holographic CDMA, wireless indoor optical CDMA, all-optical synchronization, and applications of erbium-doped fiber amplifiers (EDFAs) in optical systems. Prof. Salehi is an Associate Editor for Optical CDMA of the IEEE TRANSACTIONS ON COMMUNICATIONS since May 2001. In September 2005, he was elected as the Interim Chair of the IEEE Iran Section. He was the recipient of several awards including the Bellcore's Award of Excellence, the Nationwide Outstanding Research Award from the Ministry of Science, Research, and Technology in 2003, and the Nation's Highly Cited Researcher Award in 2004. In 2007 he received Khwarazmi International prize, first rank, in fundamental research and also the outstanding Inventor Award (Gold medal) from World Intellectual Property Organization (WIPO), Geneva, Switzerland. He is among the 250 preeminent and most influential researchers worldwide in the Institute for Scientific Information (ISI) Highly Cited in the Computer-Science Category. He is the corecipient of the IEEE's Best Paper Award in 2004 from the International Symposium on Communications and Information Technology, Sapporo, Japan.